NASA TECHNICAL MEMORANDUM

NASA TM X-1688

NASA TM X-1688

19960411 002

A STUDY TO DETERMINE THE PRESENCE OF VOLTAGE BREAKDOWN DUE TO PROTON IRRADIATION IN POLYMERIC MATERIALS

DEPARTMENT OF DEFENSE
PLASTICS TECHNICAL EVALUATION CENTER
PICATINNY ARSENAL, DOVER, N. J.

by Herbert D. Hendricks and William E. Miller

Langley Research Center
Langley Station, Hampton, Va.

DISTRIBUTION STATEMENT A
Approved for public release;
Distribution Unlimited

NATIONAL AERONAUTICS AND SPACE ADMINISTRATION • WASHINGTON, D. C. • NOVEMBER 1968

58711

DISCLAIMER NOTICE

THIS DOCUMENT IS BEST QUALITY AVAILABLE. THE COPY FURNISHED TO DTIC CONTAINED A SIGNIFICANT NUMBER OF PAGES WHICH DO NOT REPRODUCE LEGIBLY.

NASA TM X-1688

A STUDY TO DETERMINE THE PRESENCE OF VOLTAGE BREAKDOWN DUE TO PROTON IRRADIATION IN POLYMERIC MATERIALS

By Herbert D. Hendricks and William E. Miller

Langley Research Center
Langley Station, Hampton, Va.

NATIONAL AERONAUTICS AND SPACE ADMINISTRATION

For sale by the Clearinghouse for Federal Scientific and Technical Information
Springfield, Virginia 22151 – CFSTI price $3.00

DTIC QUALITY INSPECTED 1

A STUDY TO DETERMINE THE PRESENCE OF VOLTAGE BREAKDOWN DUE TO PROTON IRRADIATION IN POLYMERIC MATERIALS

By Herbert D. Hendricks and William E. Miller
Langley Research Center

SUMMARY

A study was made to determine proton-induced voltage breakdowns in a series of polymeric materials: Kapton (H-film), Teflon (TFE), Pyrrone, Mylar, and polyethylene. Proton energy was varied from 0.40 to 3.25 MeV with a flux of 10^9, 10^{10}, 10^{11}, or 2×10^{11} protons/cm^2-sec. Samples were irradiated to a fluence of 10^{13} to 5×10^{14} protons/cm^2 for each test. Sample temperatures were 27° C and -134° C. No charge storage or induced voltage-breakdown effects were observed. This observation is in sharp contrast to the numerous induced voltage breakdowns observed for electron irradiation of similar types of polymeric samples. A theory developed by Nichols and van Lint predicts that a behavior of this type should be less prevalent because of proton rather than electron irradiation.

INTRODUCTION

Induced voltage breakdown due to electron irradiation in polymeric materials has been investigated (refs. 1 to 3); however, the effects of proton irradiation in producing voltage breakdown in polymeric materials has not been investigated. An evaluation of proton effects is necessary because of the abundance of protons found in the cislunar space-radiation environment (ref. 4). In most spacecraft, there is an abundance of dielectric material used for various purposes such as sensors, coatings, antenna components, structural members, and insulation for wires. Spurious signals causing abnormal operation of the satellite could be introduced into critical control circuits by protons of the type found in cislunar space.

The purpose of this study is to determine the effects of proton-irradiation-induced voltage breakdown on five polymeric materials: Kapton (H-film), Teflon (TFE), Pyrrone, Mylar, and polyethylene. The chemical names and some physical properties of these materials are given in table I. These materials are chosen because of their wide range of applications; also, data are available on electron-induced voltage breakdown and a comparison can be made. The proton energy varies from 0.40 to 3.25 MeV (approximately 0.1 to 2.0 times the range of protons in the polymers), and the proton flux varies from

10^9 to 2×10^{11} protons/cm^2-sec. A number of samples of these materials are irradiated with protons to a fluence of 10^{13} to 5×10^{14} protons/cm^2 at temperatures of 27° C and -134° C. Samples are prepared in the form of planar capacitors and are monitored during and after irradiation for voltage breakdowns. Samples are tested with and without a bias voltage. The results of these tests are presented.

A brief discussion is presented of a theory by Nichols and van Lint (ref. 5) concerning the transient response of insulators to irradiating particles. The approach by Nichols and van Lint was to consider the different nature of the paths of electrons which have been removed from the parent atom by the primary radiation. The theory was developed to show the influence of the generation of electron-ion pairs by different types of radiation (electrons and protons) and the resulting behavior within the dielectrics. Many other aspects concerning the electrical behavior of dielectrics due to radiation were also developed.

APPARATUS AND TESTS

Accelerator Systems

The polymer samples were irradiated with protons from Van de Graaff proton accelerators of the type described in reference 6. Protons with incident kinetic energies from 0.40 MeV to 3.25 MeV were used. The accelerators were calibrated with the aid of proton-gamma and proton-neutron reactions, the proton-gamma reaction occurring in fluorine at a proton energy of 341 keV, and the proton-neutron reaction occurring in lithium at a proton energy of 1.88 MeV. The energy of the accelerators was further confirmed with an energy analyzing magnet and a nuclear-magnetic-resonance unit to determine the effective magnetic field for bending a proton of a given energy. Accelerator energy calibration was also checked in the electron mode by using semiconductor detectors and radioactive isotopes for standards. The energy values determined by these different methods agreed within ±2 keV.

Protons from the accelerators pass through an evacuated drift tube into an energy analyzing magnet (Mass × Energy = 16). The protons are bent through an angle of 45° and exit through a feedback slit system which controls the energy variations of the accelerator (fig. 1). The proton beam then enters a two-dimensional electrostatic scanner which scans the proton beam horizontally and vertically over the target area located in the test chamber.

Test Chamber

The test chamber shown schematically in figure 1 was maintained during tests to a pressure less than 6.65×10^{-4} N/m^2. The beam-current uniformity and density were

determined by a Faraday cup array (fig. 2) mounted in the chamber on a rotatable arm. Each sample was mounted on a liquid-nitrogen heat sink which was attached through the top wall of the chamber. The sample holder also contained a Faraday cup to monitor the proton beam while the test was being performed.

Beam-Current Density and Uniformity

The proton-beam pattern was determined by a Faraday cup array (fig. 2) mounted in the test chamber. During this series of tests, the values registered by individual Faraday cups varied less than ±10 percent from the average of all the Faraday cups in the array. A telephone stepping relay was used to switch the output from each of the 24 Faraday cups into the input of an electrometer used to measure the proton-beam current. The beam-current density was also determined by this system. The Faraday cup array and the sample Faraday cup were all biased 100 volts negative to remove effects of current loss due to secondary electron production.

Test Samples

The polymer samples of Kapton (H-film), Teflon (TFE), Mylar-C and Mylar-A, and polyethylene were obtained from commercial manufacturers. The Pyrrone samples were obtained from NASA Langley Research Center personnel who developed this polymer (ref. 7). The physical properties of the materials are listed in table I.

All test samples were made in the form of a planar capacitor as shown in figure 3. Aluminum was vapor deposited on each side of a polymer sample to a thickness of approximately 1750 angstroms. The aluminum thickness was determined by a Fizeau-Tolansky-type interferometer and was further monitored during each process by frequency changes on a thin-film monitor. This particular thickness was chosen as a minimum after tests showed that a thinner layer gave a higher surface resistance across the sample (on the order of 2 to 10 ohms).

The sample (fig. 3) was mounted on an aluminum plate (figs. 2 and 4) with an area of 5 cm by 5 cm exposed to the proton beam. The front side of the sample, which was covered entirely by vapor-deposited aluminum, was attached to the rear of the mounting plate by use of a conducting silver-loaded epoxy to give better thermal contact to the frame. An aluminum frame was placed over the part of the rear surface of the polymer film that did not have a coating of aluminum to insure good thermal contact.

Prior to evaluation of the samples, temperature profiles on the front and back of the sample were taken. The profile indicated a lower temperature toward the sides near the contact with the frame (-191° C), and the single rear thermocouple indicated -134° C. After 1 hour in a pressure of less than 6.65×10^{-4} N/m^2, the samples were cooled below -134° C.

Table II shows the range of resistance and capacitance of the samples before and after mounting, cooling, and radiation evaluation tests.

Test Circuit

For all tests, the samples were mounted as shown in figure 2. When the front of the sample was at ground potential, the rear of the sample was used to monitor voltage-breakdown signals. Electrical connection to the rear of the sample was made by means of a spring-loaded mechanical contact attached as shown in figures 2 and 4. The schematic of the test circuit is shown in figure 5. After contact was made to the rear of the sample, a shielded coaxial cable was then connected either directly to a storage oscilloscope (direct couple, with a 1-megohm input impedance) or through a 50-volt battery network which was used to apply positive bias to the rear of the sample. The storage oscilloscope was then used to detect any voltage breakdowns induced in the samples. The oscilloscope sensitivities used during the tests for voltage breakdowns were 0.1 to 0.5 V/cm vertical and 1.0×10^{-6} to 2.0×10^{-1} sec/cm horizontal.

The test pulser circuit shown in figure 6 was used to check the detection circuit to insure proper operation. By charging a capacitor in the circuit to a given voltage and then discharging it into the input of the test circuit, the detection circuit could be checked for proper response. The test pulser gives a sharp-rise time pulse with a maximum voltage corresponding to the charging voltage and a discharge curve dependent on the resistance-capacitance time constant of the circuit into which the capacitor is discharged. Because all test samples had a capacitance of a few nanofarads, a 5-nanofarad capacitor was used to test the circuit response.

Test Procedures

After the samples were vapor deposited with aluminum on both sides, they were attached to an aluminum plate. The samples were checked for resistance and capacitance after curing of the silver-loaded epoxy. If the values of resistance and capacitance were of the order of those listed in table II for the various materials, the sample was accepted for testing. The sample was then mounted in the test chamber as shown in figures 2 and 4. The test chamber was then evacuated to a pressure of less than 6.65×10^{-4} N/m^2 and another check of the resistance and capacitance of the sample was made. If the check was suitable, a test of the operation of the detection circuit was made with the test pulser. For tests made below room temperature (less than -134° C), the liquid-nitrogen heat sink was filled. When a thermocouple attached to the outer edge of the sample holder (fig. 2) indicated -191° C, the test with proton irradiation was started.

The accelerator was turned on and the beam was projected onto the Faraday cup array. After a check for acceptable beam uniformity (±10 percent) and current density,

the Faraday cup array was removed from in front of the sample and the monitoring of the sample started. The current density would then be monitored by the Faraday cup located under the sample (figs. 2 and 4). The proton flux was 10^9, 10^{10}, 10^{11} or 2×10^{11} protons/cm^2-sec. The total fluence for each sample was between 10^{13} and 5×10^{14} protons/cm^2 (table III), which is equivalent to approximately 1 to 10 years exposure in cislunar space. During each run, the rear of the sample was continuously monitored for induced voltage breakdown by observing a storage oscilloscope.

The polymer film samples were irradiated with protons of energies equivalent to approximately 0.1, 0.5, 1.0, and 2.0 times the range of protons for a given sample thickness. (The method for calculating range-energy relations for various materials is discussed in the appendix.) The proton energies were chosen to give a fairly wide range of proton distributions within the samples, thus insuring that the variable-energy parameter would be explored. Table III gives the proton energies, fluxes, fluences, and temperature parameters studied for the various polymeric materials.

RESULTS AND DISCUSSION

In all cases for each polymeric material studied over the range of proton energies and proton fluxes evaluated, no voltage breakdowns were observed with the system used in this series of tests (including the samples which were biased). This observation is in direct contrast to results obtained from electron irradiation of samples tested in an almost identical manner. The voltage breakdown in polymers induced by electron irradiation appears to be due to trapping of charge carriers and the resultant charge storage and buildup of charge (refs. 1 and 2). Both theory (refs. 2 and 3) and experiment (refs. 1 to 3) indicate that the breakdowns depend on the sample temperature, the electron energy, and incident flux. The absence of dielectric breakdown from proton irradiation may be due to the heavy ionization tracks produced by the bombarding particles. Protons are known to be densely ionizing particles; whereas, electrons are lightly ionizing particles. Thus, irradiation by high-energy electrons would generate relatively isolated electron-ion pairs; whereas, protons create dense paths of electron-ion pairs, the behavior of which is influenced by the presence of the adjacent electrons and the high local fields set up by the ions. Therefore, the densely ionized paths created by the protons enhance the probability of electron-ion recombination and eliminate charge buildup due to trapping of charges. A theory by D. K. Nichols and V. A. J. van Lint (ref. 5) discusses the fact that transient effects will typically be less for protons than for electrons. This theory (ref. 5) describes electron trapping processes, energy deposition by particles, ionization cross section, charge diffusion, charge drift rate, volume charge density, and other parameters that could influence transients produced in dielectrics. The theory presented by Nichols and van Lint predicting a less transient response in dielectrics irradiated with protons

rather than electrons is supported for the parameters and materials investigated and presented in this paper and in references 1 and 2. (See table III.)

The ranges of the resistance and capacitance values of the samples obtained before and after irradiation are given in table II. No change greater than the accuracy of the impedance bridge was detected for all samples after irradiation. During the series of tests at 400 keV, a Teflon (TFE) sample was exposed at a flux of 2×10^{11} protons/cm^2-sec to a fluence of 5×10^{14} protons/cm^2. No proton-induced voltage breakdowns were observed. However, the specular reflecting aluminum on the front surface of the sample became diffuse. A similar test was made by using strips of Mylar-A, Mylar-C, Kapton (H-film), and another Teflon (TFE) as the samples. The aluminum surfaces on the Mylar and Kapton (H-film) samples remained unchanged; whereas, the aluminum surface on the Teflon sample became diffuse. This diffusion is thought to be due to gas evolution from the Teflon. Further tests showed the Teflon samples to be flux and fluence dependent. When Teflon samples were run at a lower flux (10^{11} protons/cm^2-sec) to the same fluence (10^{14} protons/cm^2), the surface was hardly changed. However, when the flux was increased to 2×10^{11} protons/cm^2-sec, the surface became more diffuse. However, after irradiating the samples at the lower flux to a higher fluence (such as, 5×10^{14} protons/cm^2), the surface again became diffuse.

CONCLUDING REMARKS

During the present study of proton-induced voltage breakdowns in polymeric materials (Kapton (H-film), Teflon (TFE), Pyrrone, Mylar, and polyethylene), the conditions previously found to cause voltage breakdown in samples irradiated with electrons were investigated. However, no induced voltage breakdowns were detected during the tests with proton irradiation. At these proton energies, fluxes, and fluences, a large recombination of trapped charges appears to take place and thus eliminates the type of effect previously observed during tests with electron irradiation. A theory by Nichols and van Lint predicts such a behavior. Proton irradiation of Teflon samples at high fluxes and to a high fluence produces a diffuse surface.

Langley Research Center,
National Aeronautics and Space Administration,
Langley Station, Hampton, Va., June 19, 1968,
124-09-12-01-23.

APPENDIX

PROTON RANGE-ENERGY RELATIONS FOR SOME SELECTED MATERIALS

Proton range-energy relations for Kapton (H-film), Lucite, polyethylene, Saran, anthracene, Teflon, carbon, Pyrrone, and Mylar are shown in figure 7. The data for Lucite, polyethylene, Saran, anthracene, Teflon, and carbon were taken from reference 8. The data for Mylar were taken from reference 9. Because the proton range-energy relations for Kapton (H-film) and Pyrrone were not available in any published literature, they were computed by a method given in reference 9.

In order to calculate the range of energetic protons in Kapton (H-film) and Pyrrone, the ionization potential I and the ratio of atomic number to atomic mass Z/A for each material must be found. The ionization potential was found by using the formula (from ref. 8)

$$\ln I = \frac{\sum_i f_i Z_i \ln I_{adj_i}}{\sum_i f_i Z_i}$$

where

f_i fraction of ith constituent

Z_i atomic number of ith constituent

I_{adj_i} adjusted ionization potential of ith constituent, electron volts

The ratio Z/A was found by using the formula (from ref. 9)

$$\frac{Z}{A} = \frac{1}{\rho} \sum_i \rho_i \frac{Z_i}{A_i}$$

where

ρ density, $\sum_i \rho_i$

ρ_i partial density of ith constituent

A_i atomic mass number of ith constituent

APPENDIX

The values I and Z/A computed for Kapton (H-film) and Pyrrone were then used in the "Two Variable Range Table" in reference 9 to obtain the proton range-energy relations for these materials.

The accuracy of the calculated range was estimated to be ±5 percent because of chemical binding effects.

The method used for these calculations is considered to be reliable and could easily be used for proton range-energy calculations of other compounds and mixtures such as ceramics and alloys.

REFERENCES

1. Storti, George M.; Phillips, Donald H.; and Frank, Clifford S.: Experimental Study of Transient Effects in Dielectric Materials Caused by Electron Irradiation. NASA TN D-3032, 1965.

2. Storti, George M.: Experimental Investigation and Analysis of Dielectric Breakdowns Induced by Electron Irradiation in Polymer Films. NASA TN D-4810, 1968.

3. Monteith, L. K.; Hauser, J. R.; and Royal, T. M.: Charge Storage Effects in Mylar Resulting From Electron Irradiation. NASA CR-656, 1966.

4. Vette, James I.: Models of the Trapped Radiation Environment. Volume I: Inner Zone Protons and Electrons. NASA SP-3024, 1966.

5. Nichols, D. K.; and van Lint, V. A. J.: Theory of Transient Electrical Effects in Irradiated Insulators. IEEE Trans. Nucl. Sci., vol. NS-13, no. 6, Dec. 1966, pp. 119-126.

6. Livingston, M. Stanley; and Blewett, John P.: Particle Accelerators. McGraw-Hill Book Co., Inc., 1962, pp. 14-72.

7. Pezdirtz, George F.; and Bell, Vernon L.: An Exploratory Study of a New Class of Stepladder and Ladder Polymers-Polyimidazopyrrolones. NASA TN D-3148, 1965.

8. Janni, Joseph F.: Calculations of Energy Loss, Range, Pathlength, Straggling, Multiple Scattering, and the Probability of Inelastic Nuclear Collisions for 0.1- to 1000-MeV Protons. AFWL-TR-65-150, U.S. Air Force, Sept. 1966. (Available from DDC as AD 643837.)

9. Barkas, Walter H.; and Berger, Martin J.: Tables of Energy Losses and Ranges of Heavy Charged Particles. NASA SP-3013, 1964.

TABLE I.- PHYSICAL AND CHEMICAL PARAMETERS
OF POLYMERIC MATERIALS EVALUATED

Sample type	Chemical name	Chemical formula	Nominal density, g/cm^3	Thickness range, mm	Nominal thickness, mm
Kapton (H-film)	Poly(N,N'-(p,p'oxydiphenylene) pyromellitimide	$C_{22}H_{10}N_2O_5$	1.42	0.052 to 0.060	0.050
Teflon (TFE)	Polytetrafluoroethylene	C_2F_4	2.20	0.045 to 0.052	.050
Pyrrone (PMDA-DAB)	Polyimidazopyrrolone	$C_{22}N_4H_8O_3$	1.45	0.027 to 0.045	.030
Mylar-C	Polyethylene terephthalate (capacitor grade)	$C_{10}H_8O_4$	1.30	0.022 to 0.027	.025
Mylar-A	Polyethylene terephthalate (electrical insulation grade)	$C_{10}H_8O_4$	1.30	0.120 to 0.122	.127
Polyethylene	Polyethylene	CH_2	.92	0.047 to 0.055	.050

TABLE II.- CAPACITANCE AND RESISTANCE RANGES

OF SAMPLES EVALUATED

Sample type	Resistance, MΩ	Capacitance*, nF
Kapton (H-film)	10^5 to 10^6	3.1 to 3.3
Teflon (TFE)	1 to 2×10^5	2.2 to 2.7
Pyrrone	$>10^5$	4.9 to 6.8
Mylar-C	1 to 2×10^5	6.3 to 7.4
Mylar-A	2×10^5	1.5
Polyethylene	10^5 to 10^6	2.5

*Coaxial-cable capacitance, 2.36 nF.

TABLE III.- SAMPLE TEST PARAMETERS

Sample type	Number	Flux, protons/cm^2-sec	Bias, V	Temperature, ^oC	Proton energy, MeV	Fluence, protons/cm^2
Kapton (H-film)	30	10^9, 10^{10}, 10^{11}, 2×10^{11}	0, +50	27, -134	0.4, 1.0, 1.5, 2.5	10^{13}, 5×10^{13}, 5×10^{14}
Teflon (TFE)	20	10^9, 10^{10}, 10^{11}, 2×10^{11}	0, +50	27, -134	0.4, 1.5, 2.15	10^{13}, 10^{14}, 5×10^{14}
Pyrrone	18	10^9, 10^{10}	0	27, -134	1.0, 1.5	10^{13}
Mylar-C	10	10^9, 10^{10}	0, +50	27, -134	0.8, 1.15	10^{13}
Mylar-A	4	10^{10}	0	27, -134	2.15, 3.25	10^{13}
Polyethylene	10	10^9, 10^{10}	0, +50	27	1.15, 1.65	10^{13}

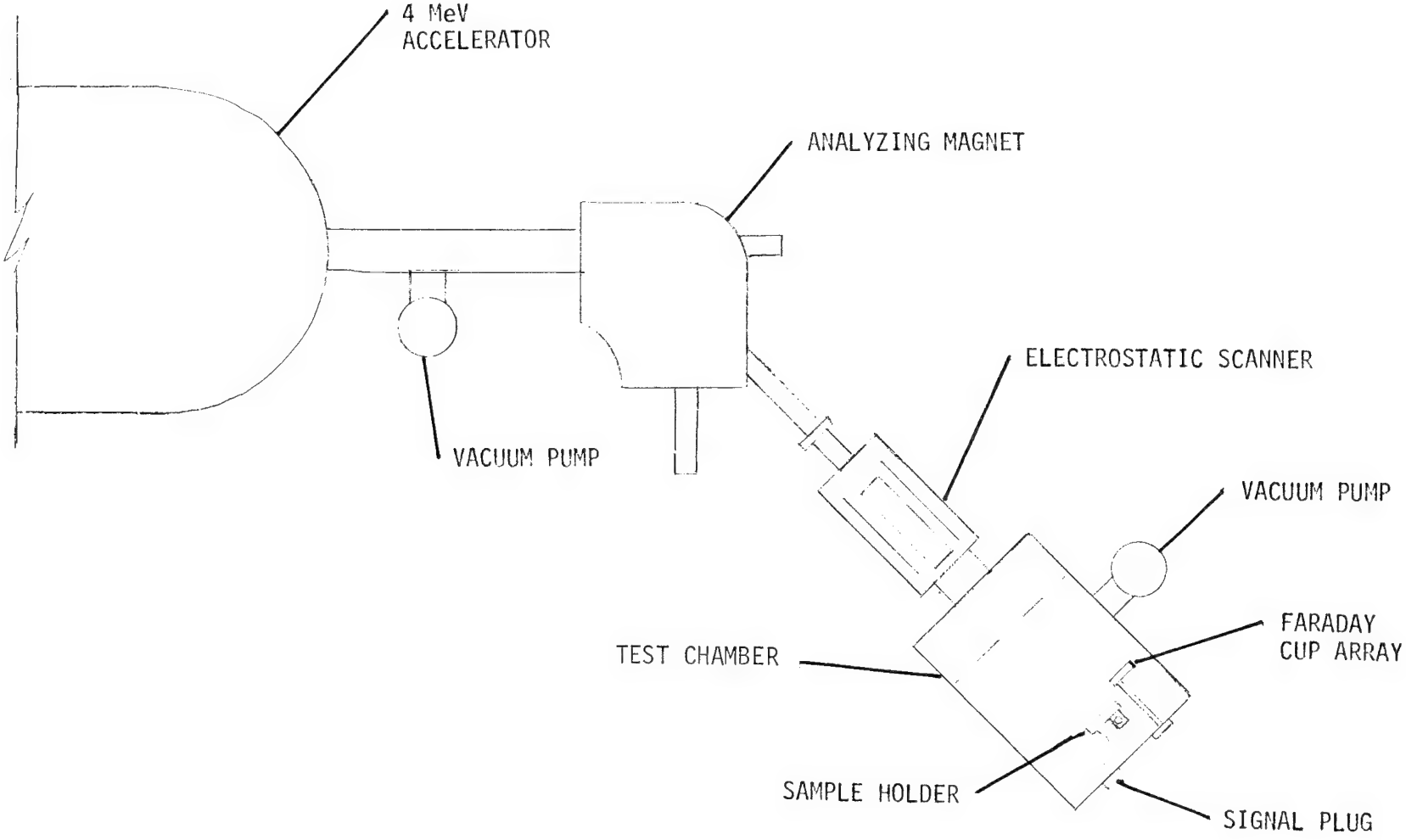

Figure 1.- Test configuration.

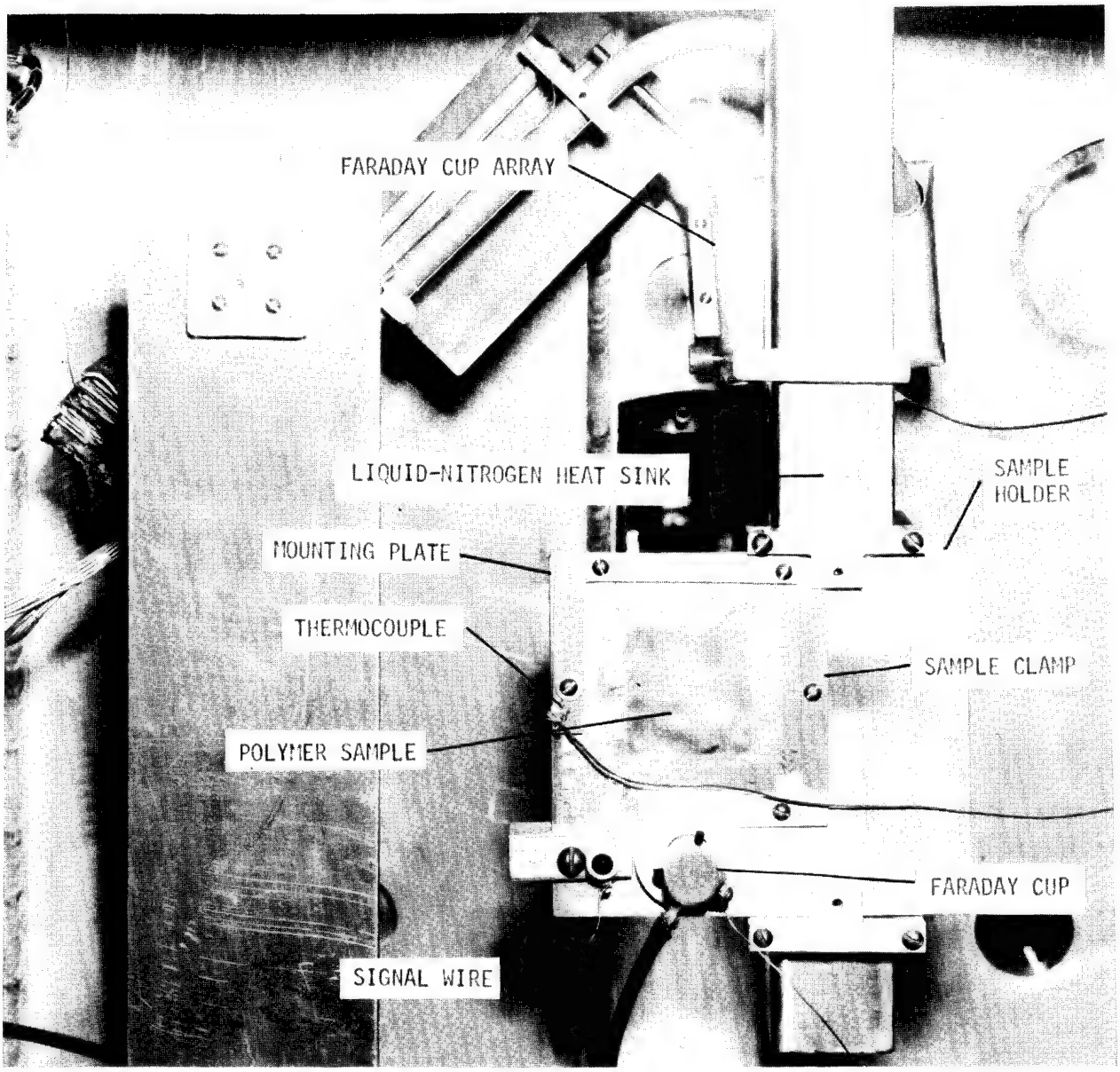

Figure 2.- Test arrangement showing rear of polymeric sample. L-68-3680

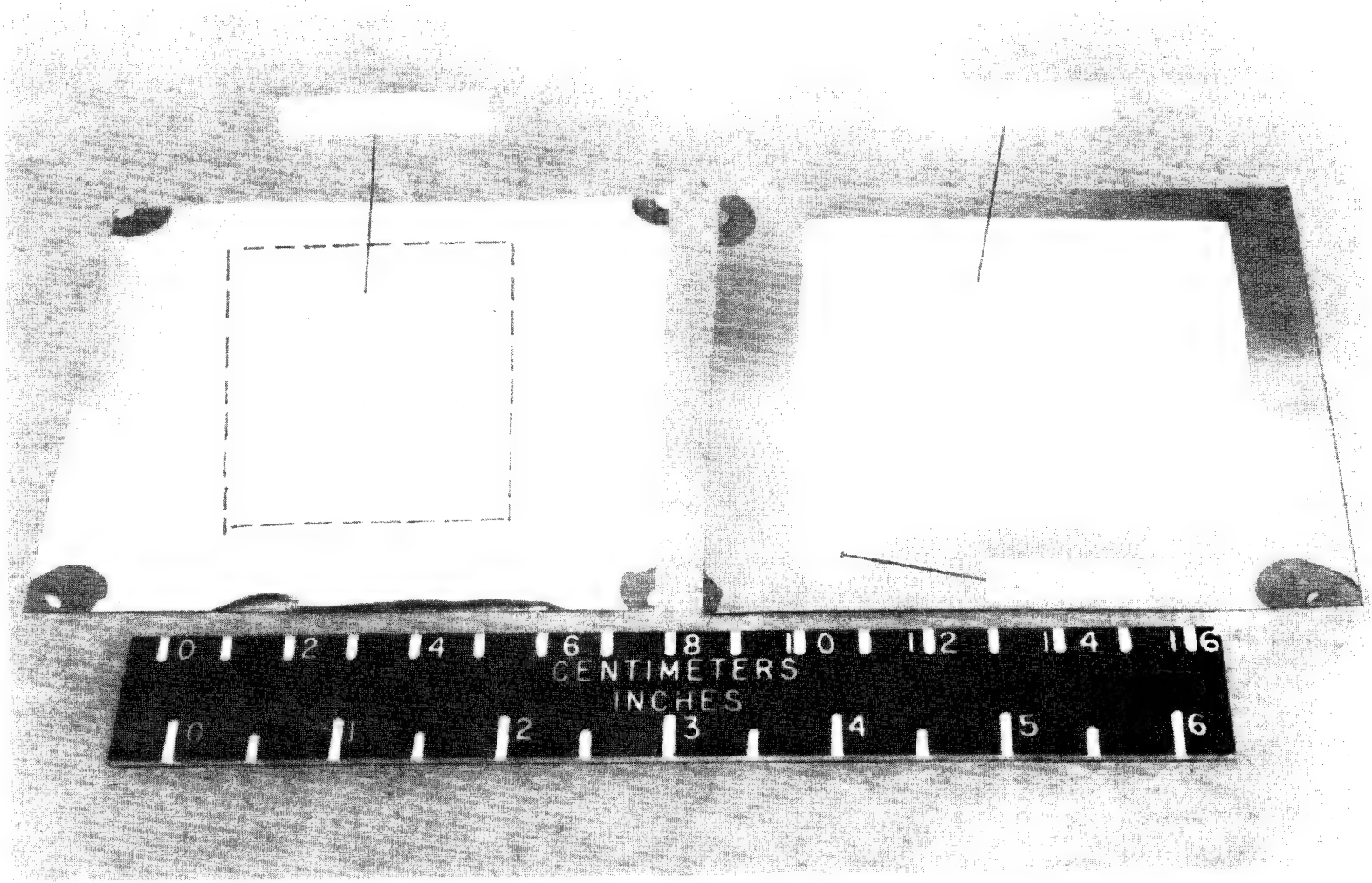
0 2 4 6 8 10 12 14 16
CENTIMETERS
INCHES
0 1 2 3 4 5 6

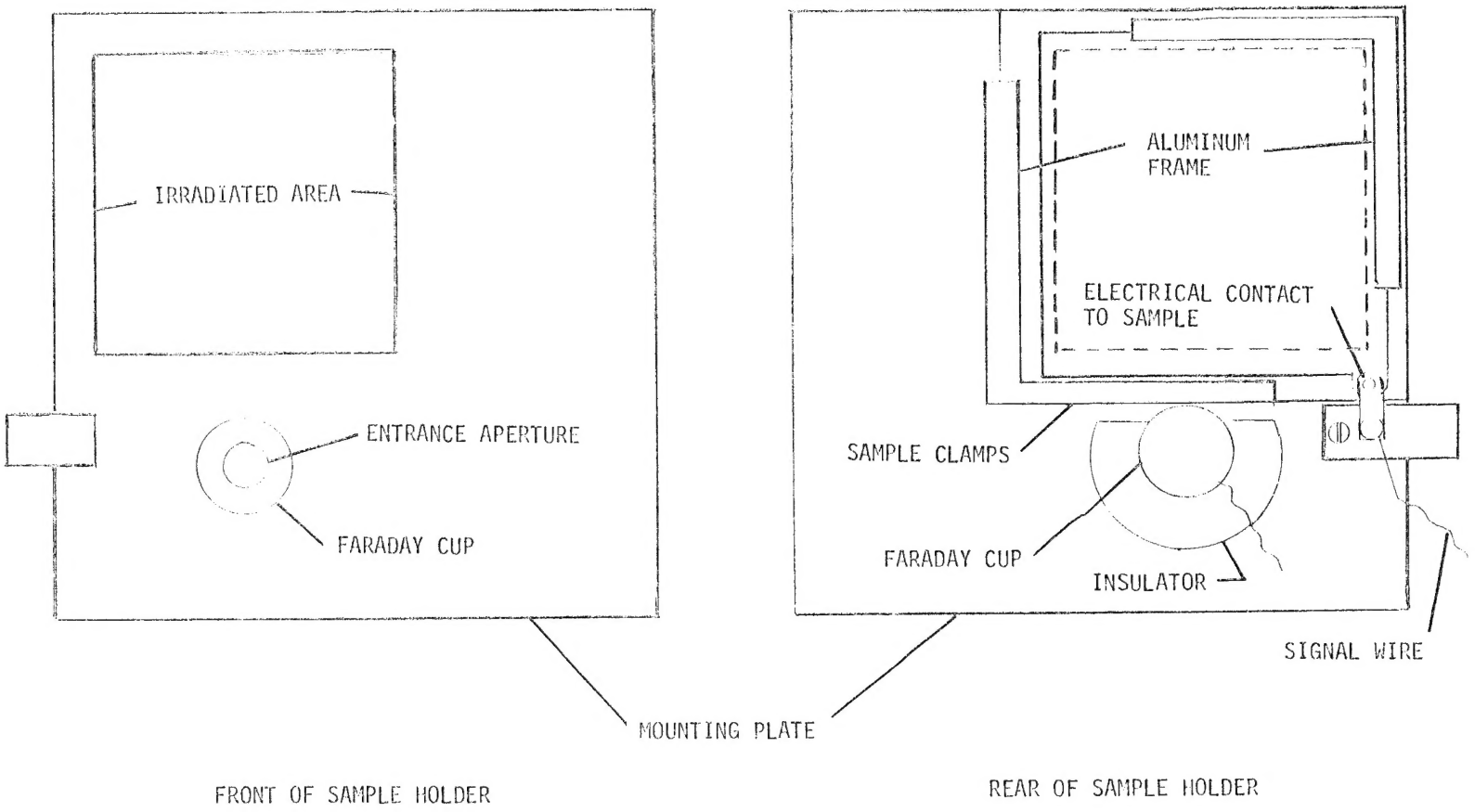

Figure 4.- Polymer-sample mounting plate with typical connections.

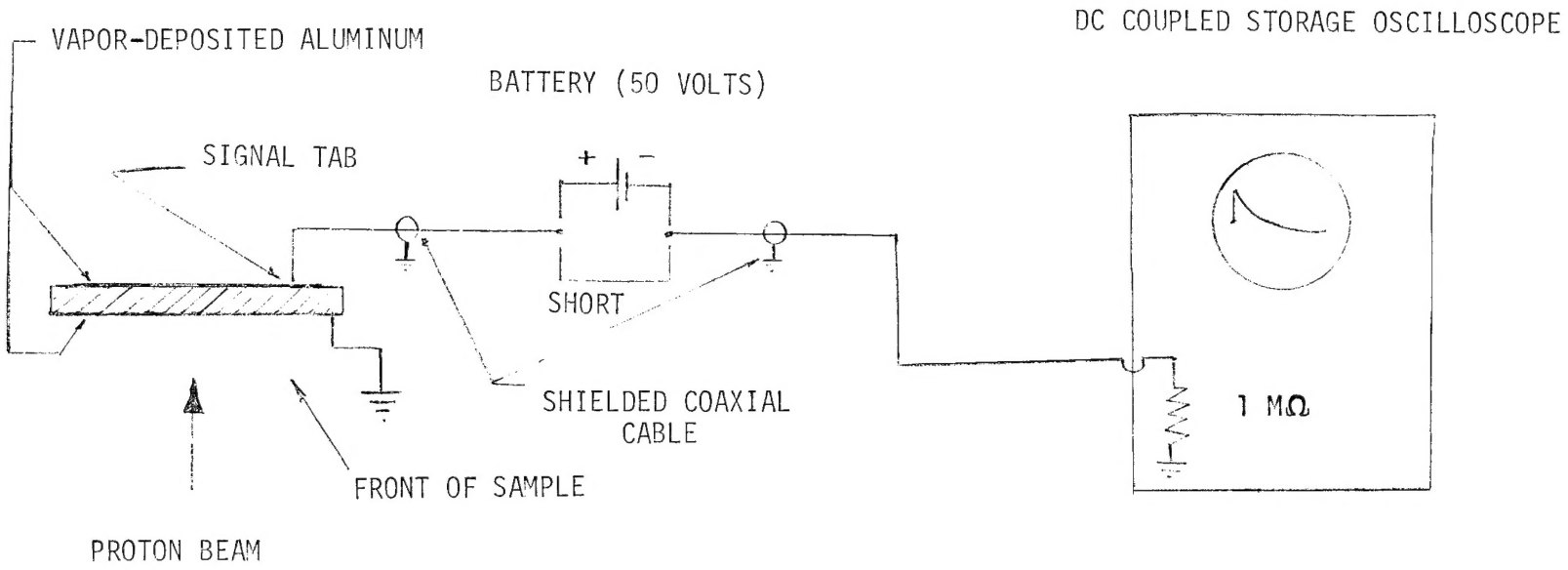

Figure 5.- Test circuit used for detecting voltage breakdowns in polymeric material.

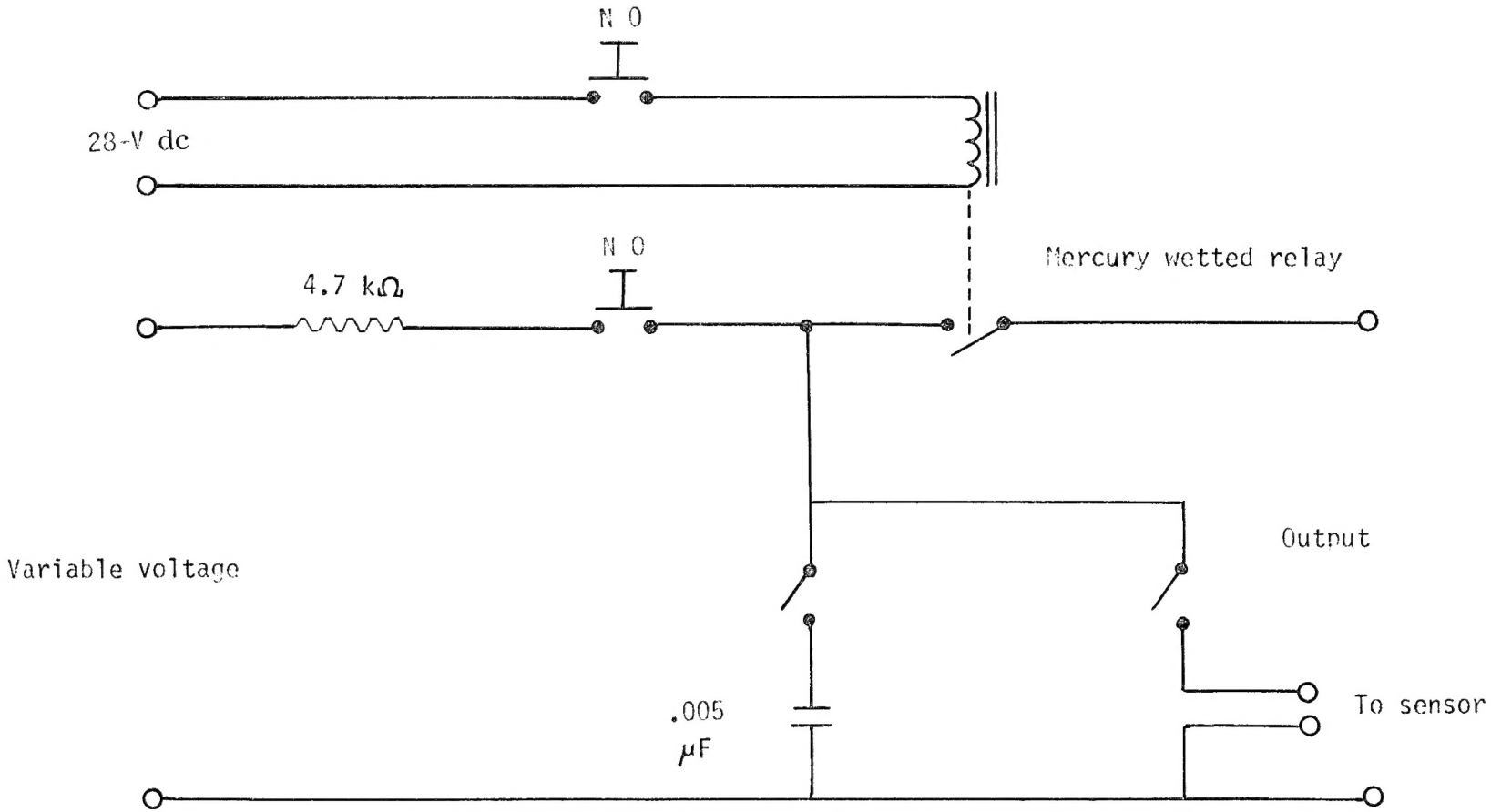

Figure 6.- Test pulser circuit used for checking voltage-breakdown detection circuit.

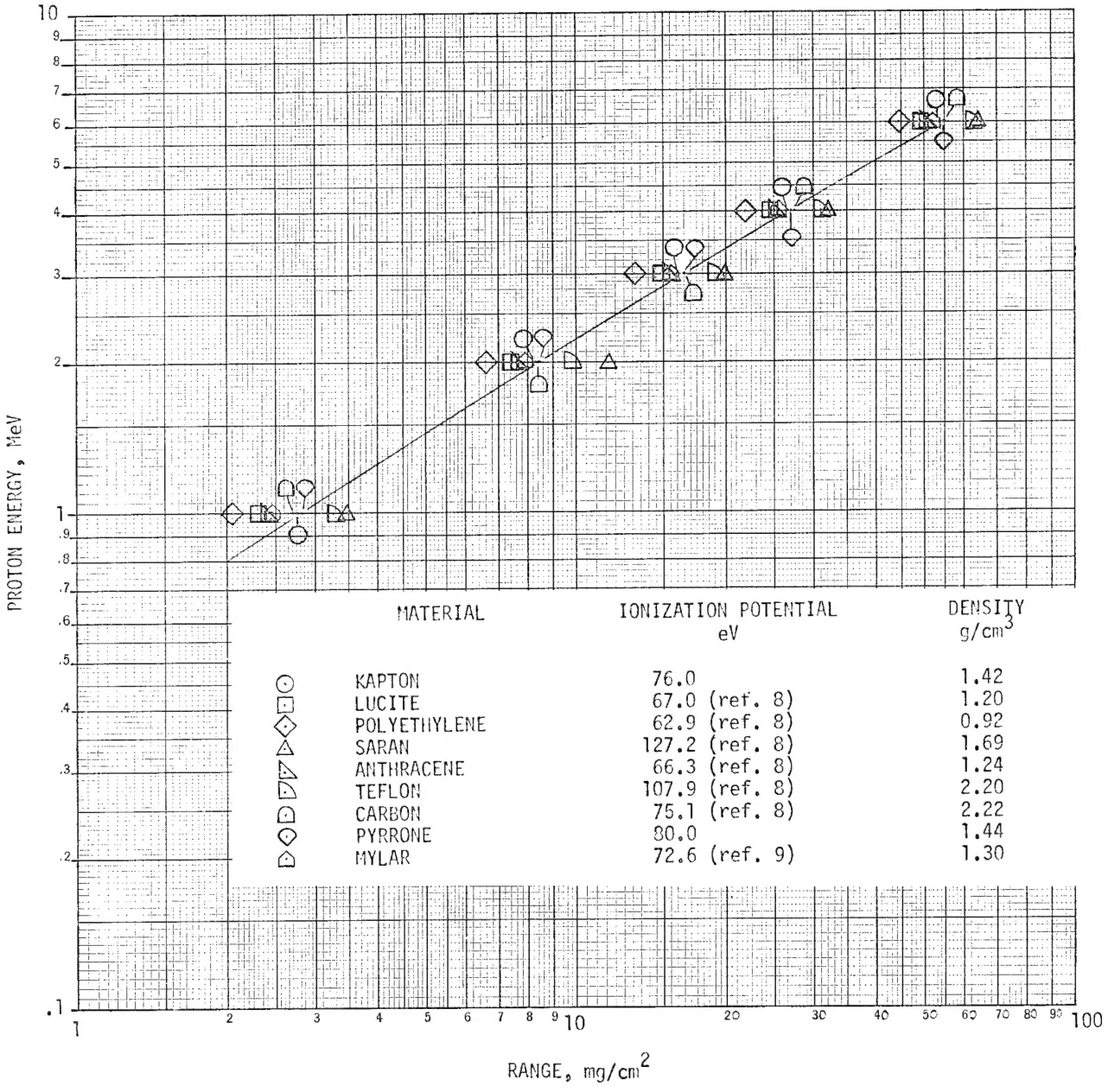

Figure 7.- Proton range-energy relations for some selected materials.